Depth Dependence and Mass Transport of Recirculating Midlatitude Gyres

NICHOLAS M. J. HALL*

Space and Atmospheric Physics Group, Imperial College, London, United Kingdom

(Manuscript received 29 June 1989, in final form 18 December 1990)

ABSTRACT

The northwest corners of the major ocean basins are characterized by seaward jets, flanked by tight, nonlinear gyres exhibiting closed potential vorticity contours. At deep levels, isolated from surface forcing, areas of homogeneous potential vorticity are apparent. A model is presented describing these "recirculation" regions, extending the quasi-geostrophic layer models of Marshall and Nurser to the continuously stratified two-dimensional case.

The study is diagnostic, concentrating on numerical inversions of idealized quasi-geostrophic potential vorticity distributions in a vertical, meridional section through a free inertial gyre. An iterative approach is used to find the "bowl" of the circulation: the free boundary between the deep recirculating homogenized water and the stagnant water below.

It is shown that the homogenized recirculation has a finite depth penetration, possibly not extending to the ocean floor. In cases where the flow reaches the bottom, the recirculation can be divided into two regions: a "core" region, where bottom currents exist and a baroclinic "fringe" to the south. The surface intensified part of the eastward jet is recirculated in the broad, westward flowing fringe, while the component of the transport returned within the core itself is largely depth independent. The enhanced mass transport of the Gulf Stream can be accounted for by the model. Its magnitude is sensitive to the upper-level potential vorticity imposed. For realistic parameters, the core carries the greater proportion of the transport.

The structure of the recirculation is dependent on the value assumed for the deep homogeneous potential vorticity. If a positive deep potential vorticity anomaly is imposed, the upper-level gyre interface moves northward while a cyclonic gyre becomes dominant in the abyssal flow. If the anomaly exceeds a certain limit, solutions can no longer be found.

1. Introduction

Recently, a number of theoretical models has been put forward, attempting to explain some of the observed features of recirculating current systems such as the Gulf Stream's seaward extension. The enhanced mass transport in such regions has been attributed to the existence of free inertial gyres which are able to spin up to far greater intensity than the wind-driven Sverdrup circulation of the interior.

The classical example of such a gyre is the model proposed by Fofonoff (1954), in which nonlinear terms allow absolute vorticity contours to depart from latitude lines and follow streamlines. Observations of the potential vorticity, q, of the world's oceans (Keffer 1985, see Fig. 1) show the existence of just such closed q contours in tight recirculating gyres adjacent to the Gulf Stream front. At levels deep enough to be isolated from surface forcing, Keffer's maps show extensive areas of homogeneous potential vorticity. This feature is also very apparent in the subsurface layers of eddy resolving numerical models (see Holland et al. 1984). Such pools of uniform q are thought to be a consequence of downgradient transfer of q by geostrophic eddies within closed streamlines in regions isolated from surface forcing (Rhines and Young 1982a). Unforced deep waters can be brought into motion through the influence of a strongly circulating upper layer (or thermocline) as shown in the simple quasi-geostrophic model of Rhines and Young (1982b).

Marshall and Nurser (1986, hereafter MN) exploit this idea in the inertial limit and generalize the Fofonoff gyre to a multilayered baroclinic ocean. The upper layer has a very low value of potential vorticity, characteristic of thermocline waters which flank the Gulf Stream where strong winter convection destroys the upper stratification, creating a wedge of low q "mode" water (see McCartney 1982). In this region there is a depression in the main thermocline, which in turn allows the abyssal potential vorticity contours to close off. In the presence of these closed contours, the abyssal recirculation can be excited through the eddy homogeni-

* Current affiliation: Department of Meteorology, University of Reading, Reading, U.K.

Corresponding author address: Dr. Nicholas M. J. Hall, University of Reading, Dept. of Meteorology, 2 Earley Gate, Whitenights, P.O. Box 239, Reading RG6 2AU, U.K.

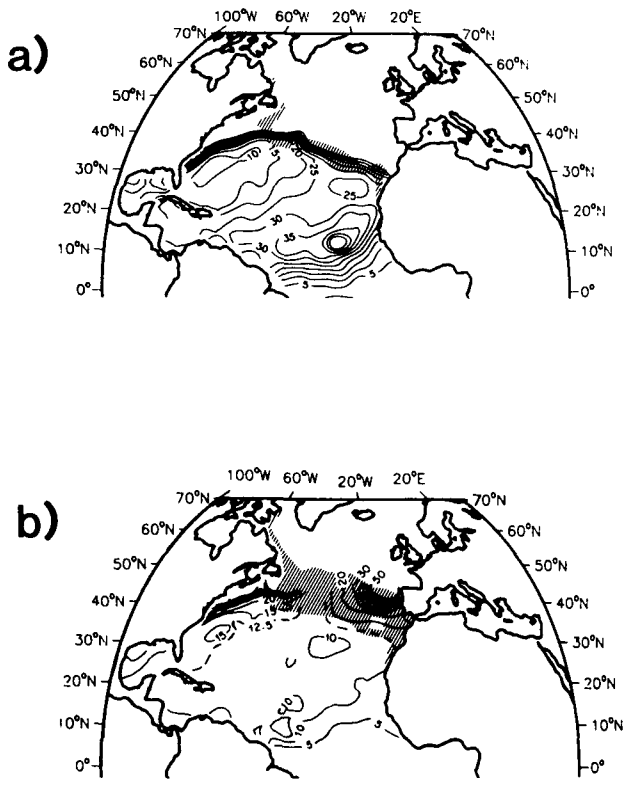

FIG. 1. North Atlantic potential vorticity taken from Keffer (1985): (a) in the $\sigma_\theta = 26.3$–26.5 layer showing closed contours; (b) in the $\sigma_\theta = 26.5$–27.0 layer, showing homogeneous regions.

zation of potential vorticity. The resulting description of the vertical structure of these free inertial gyres compares well with hydrographic sections taken across the Gulf Stream's seaward extension.

A feature of the solution is the form of the interface between the deep recirculating, constant q water and the stagnant water below (the "bowl" of the circulation). Marshall and Nurser show that their stacked Fofonoff gyres progressively shrink toward the latitude of the eastward jet with increasing depth. If the deep flow penetrates to the ocean floor, then the possibility of barotropic (depth independent) flow arises, north of where the bowl strikes the bottom. This has been explored by Greatbatch (1987), Marshall and Nurser (1988, hereafter MN2) and Cessi (1988). In the vertically continuous model of Greatbatch (1987) and the layer model of MN2, vortex stretching is an important process in controlling the extent of this barotropic region. Cessi, on the other hand, emphasizes the barotropic "core" of the recirculation, with relative vorticity balancing the beta effect, and the mass transport is predicted in terms of the value of the upper layer q, or the meridional extent of this core region.

In this paper we present an extension of MN's multilayer model to a vertically continuous one including the full effects of relative vorticity. The problem is solved by imposing the quasi-geostrophic potential vorticity field and numerically inverting an elliptic equation. A free boundary, the bowl, marks the depth to which the circulation penetrates. The position of this boundary is determined by iteration, minimizing the local geostrophic energy. In this way, the shape of the bowl can be studied in detail and the structure and strength of the flow assessed quantitatively, without the limitations of crude vertical resolution. It will be seen that the recirculation is likely to extend to the ocean floor and that both the total transport and the partition between barotropic and baroclinic transports are controlled by the upper-level potential vorticity and the stratification.

An introduction to the model is given in section 2 in the form of a review. Its continuous nature is discussed and the method of solution outlined. The results obtained from numerical inversions are presented in section 3, which also includes some comparisons with simple theory. The relative importance of vortex stretching and relative vorticity is discussed, and we investigate the way in which the strength of the gyre is determined by the parameters chosen. In section 4, the consequences of varying the value of q to which the deep water homogenizes are investigated. It is shown that the strength and position of the abyssal flow is sensitive to the value of the deep homogeneous q, and over a realistic parameter range, there is a limit on this value, beyond which solutions cannot be found. Conclusions and a summary are presented in section 5.

2. The model

a. *Fofonoff gyres*

The flow in the recirculating gyres under consideration is described by the potential vorticity equation:

$$\frac{\partial q}{\partial t} + J(\psi, q) = \mathcal{F} - \mathcal{D} \tag{1}$$

where ψ is a streamfunction, q is the quasi-geostrophic potential vorticity and $J(\psi, q)$ is the Jacobian of ψ and q,

$$\left(= \frac{\partial \psi}{\partial x}\frac{\partial q}{\partial y} - \frac{\partial \psi}{\partial y}\frac{\partial q}{\partial x} \right)$$

and represents the advection of q. Terms $\mathcal{F}$ and $\mathcal{D}$ are sources and sinks of potential vorticity, x is east y, north and t, time. The definition of q is given by

$$q = \beta y + \nabla^2\psi + f_0^2 \frac{\partial}{\partial z}\left(\frac{1}{N^2}\frac{\partial \psi}{\partial z}\right) \tag{2}$$

where f_0 and β are the values of planetary vorticity and its meridional gradient and N is the Brunt–Väisällä frequency. Equation (2) will be used in various forms throughout.

In a Fofonoff gyre (Fig. 2), time derivatives, forcing and dissipation are set to zero and q is a function of ψ

only. In such a steady, free solution, the strength of the flow is arbitrary, depending on the assumed functional relationship between q and ψ. As shown by Niiler (1966), if weak forcing and dissipation is allowed, the strength of the circulation and the (q, ψ) relationship can be constrained and in principle, determined for certain special forms of $\mathcal{F}$ and $\mathcal{D}$. Fofonoff, Niiler and MN adopted a linear (q, ψ) relationship:

$$q = q_0 + c\psi \tag{3}$$

where q_0 and c are constants.

It is important to realize that only certain forms of (q, ψ) relationship are consistent with the forms adopted for $\mathcal{F}$ and $\mathcal{D}$. For example, consider almost free, steady flow, in which advection of potential vorticity is balanced by weak forcing and dissipation. Now, if vorticity forcing is through an imposed wind stress curl at the surface and, within the recirculation, it is balanced by down-gradient eddy transfer of q, then we can write

$$\mathcal{F} = \frac{1}{\rho_0}\mathbf{k}\cdot(\nabla \times \vec{\tau})$$

$$\mathcal{D} = -\nabla\cdot(k\nabla q)$$

where ρ_0 is density, $\mathbf{k}$ is the vertical unit vector, $\vec{\tau}$ is the wind stress and k is a positive transfer coefficient. Substituting these expressions into (1) and integrating over a closed streamline we obtain

$$\frac{1}{\rho_0}\oint_\psi \vec{\tau}\cdot d\mathbf{l} = -\frac{dq}{d\psi}\oint_\psi k\mathbf{v}\cdot d\mathbf{l} \tag{4}$$

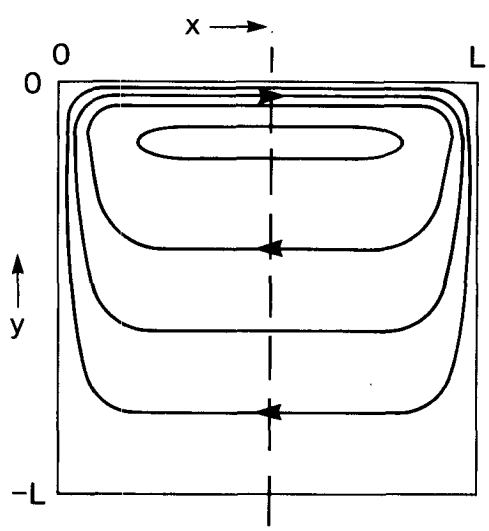

FIG. 2. Fofonoff's (1954) solution for free nonlinear barotropic flow in a rectangular basin. Weak, westward flow prevails over most of the gyre and relative vorticity is concentrated in the boundary layers and in the eastward jet to the north. The dashed meridian is a line of symmetry used as a section line in the baroclinic extensions to this solution discussed in this paper.

implying that if the sense of the circulation is to reflect the sign of the vorticity input from the wind stress then $dq/d\psi$, or c, must be negative. (In an anticyclonic gyre, with anticyclonic forcing, eddies must transport cyclonic vorticity into the gyre to maintain equilibrium. If this transfer is directed down the large-scale gradient of q, and ψ is a maximum at the gyre center then $dq/d\psi$ must be negative). However, in a barotropic Fofonoff gyre, c must be positive in order to ensure boundary layer solutions to (2). Marshall and Nurser therefore suggested that the vortex stretching term in (2) is essential if the inertial solution is to be equilibrated by downgradient eddy transfer of q with c negative. A Fofonoff gyre with this type of equilibration must have baroclinic structure. It is the precise nature of this baroclinic structure that concerns us in this paper. The constraints on $dq/d\psi$ are discussed further in section 3. Initially, however, we will concentrate on the simpler case of uniform potential vorticity in regions of flow.

b. *Vertical structure in layer models*

We are interested in the steady vertical structure of the recirculation. Accordingly the model set out in the following discussion is diagnostic, concentrating on a meridional vertical section through the center of a Fofonoff gyre, where zonal derivatives can be neglected. If the potential vorticity is specified everywhere in this section then the flow field can be obtained by inverting the elliptic operator in (2) with appropriate boundary conditions.

The structure of the thermocline and the abyssal flow beneath can be modeled most simply by imposing two values of potential vorticity in the two regions. A low value is imposed at upper levels in order to depress the thermocline and represent the mode water found in this region. Beneath the thermocline, it is assumed that q homogenizes to the value of planetary vorticity at the axis of the eastward jet. (The effects of relaxing this assumption are considered in section 4.) In the context of the barotropic Fofonoff gyre of Fig. 2 and its extension to the baroclinic case (see Fig. 3), this simply means that q is set equal to zero in the abyssal flow region. A value of $-\beta L$ is chosen for the upper layer q in the subtropical gyre (where L is the meridional extent of the gyre), to ensure continuity with planetary vorticity at the southern edge of the gyre. The corresponding value for the subpolar gyre is βL, giving a realistic front in q at upper levels near the Gulf Stream (see Fig. 1).

Figure 3 is a schematic diagram of the quasi-geostrophic layer model used in MN and MN2. Layer 1 has moving fluid, with constant low potential vorticity throughout the domain $-L \leqslant y \leqslant 0$. Its thickness increases in a linear fashion on moving northwards, as vortex stretching offsets planetary vorticity. Accordingly, the interface between layers 1 and 2 (the ther-

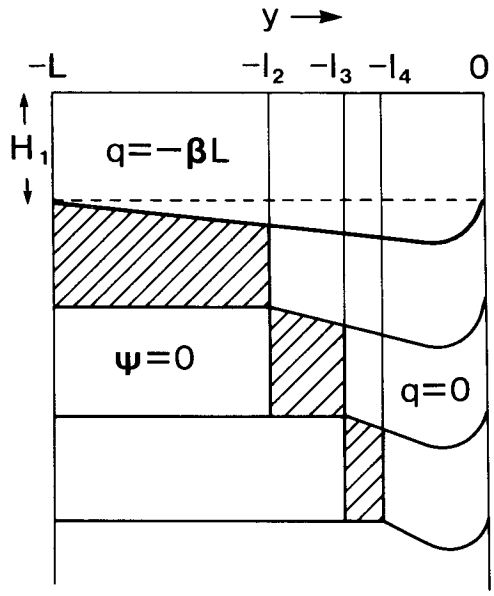

FIG. 3. The vertical structure in MN's layer model of the recirculation. Regions of vortex "squashing" are shaded to represent the bowl of the circulation. North of these regions, q is homogeneous and free flow exists.

mocline) is pushed down, progressively squashing the still motionless layer 2. Thus the potential vorticity in layer 2 increases at a faster rate than the beta effect and so q_2 reaches zero at $y = -l_2$. This marks the southern edge of the deep homogenized gyre. Contours of q_2 can now close off between this latitude and $y = 0$, and q_2 can homogenize to a zero value. To maintain $q_2 = 0$ against the background planetary vorticity gradient, layer 2 is now stretched until it regains its reference thickness at $y = 0$. This results in a depression of the interface between layers 2 and 3, implying motion in layer 2 and also squashing layer 3 and bringing it into motion at $y = -l_3$. The l_ns collectively define the bowl of the circulation. Figure 3 shows the "hyperbolic plunge" of the bowl described by MN, with the homogeneous gyres retreating northwards with depth, and the penetration of the flow extending to infinity as the axis of the eastward jet is approached. The inclusion of relative vorticity will introduce curvature to these layer interfaces and indeed it is essential in the eastward jet, where isopycnals are brought back to their reference levels at $y = 0$. To solve the problem fully, including relative vorticity, Eq. (2) can be rewritten in layer form and solved for N isopycnal layers of constant density interval as a set of N coupled equations:

$$q_1 = \beta y + \nabla^2\psi_1 + L_\rho^{-2}(\psi_2 - \psi_1) = -\beta L + c_1\psi_1$$

$$q_n = \beta y + \nabla^2\psi_n + \alpha_n L_\rho^{-2}(\psi_{n-1} - 2\psi_n + \psi_{n+1}) = 0$$

$$q_N = \beta y + \nabla^2\psi_N + \alpha_N L_\rho^{-2}(\psi_{N-1} - \psi_N) = 0 \quad (\text{or} = c_N\psi_N) \quad (5)$$

with all subsurface layers having $q_n = 0$ where there is flow. The subscript denotes layer number and L_ρ is the Rossby radius ($=\sqrt{g'H_1}/f$ where g' is the reduced gravity and H_1 is the thickness of layer 1); α_n is the ratio of the upper layer thickness to the thickness of layer n. In each abyssal layer, throughout the stagnant region south of l_n, $\psi_n = 0$.

In the MN model, interior solutions are found for the westward flowing baroclinic region far from the eastward jet, and the $\nabla^2\psi$ term is neglected. The values of l_n are found simply by matching the streamfunctions at this latitude. An alternative treatment is to retain the $\nabla^2\psi$ term in (5) and apply additional, higher order boundary conditions to locate l_n. In a two-layer model of this kind, Cessi (1988) chose to make velocity continuous, imposing $d\psi/dy = 0$ at $y = -l_2$. To satisfy this boundary condition, relative vorticity must play a role right out to this latitude, resulting in a discontinuous jump in vorticity. This "no slip" condition eliminates "extrema" of vorticity at the gyre edge which would otherwise arise (if the region to the south were considered to be truly stagnant). Such extrema are inconsistent with simple circulation integrals (for a full discussion see Cessi, et al. 1987, hereafter CIY). Marshall and Nurser point out that the inclusion of relative vorticity also modifies their solutions in terms of the depth penetration of the flow, possibly arresting it at a finite depth once the gyres have contracted to a width comparable with the scale of the eastward jet at the surface. If, however, the flow reaches the ocean floor a depth independent component to the flow can arise. The question remains as to what determines the strength of this component. Since the vortex stretching term disappears from the vertical integral of (2), the depth integrated flow must be determined entirely from the remaining terms in ψ. These arise either through relative vorticity or through nonzero values of $dq/d\psi$ (or c) appearing in the form chosen for q. In all cases, relative vorticity is essential for the closure of the circulation in the eastward jet to the north. Factors affecting the depth penetration and the depth-independent part of the recirculation will be quantified in section 3 in terms of the continuous model described below.

c. *A vertically continuous model*

To understand the vertically continuous extension of Fig. 3, it is useful to ask what would happen if the number of layers became very large. Figure 3 consists of regions of stagnation, vortex squashing and stretching. As the number of layers is increased, the squashing regions become narrower. In the continuous limit, they are replaced by a line, the bowl, along which there is a discontinuity in q. This discontinuity is not dependent on the presence of relative vorticity, as is the discontinuity which results from the application of the no slip boundary condition mentioned above. It is a

discontinuity in the vortex stretching, arising from the fact that the smooth, squashing regions found in the layer models have collapsed onto a line. This line is the boundary between motionless water, where $q = \beta y$, and recirculating water where the flow can maintain $q = 0$ through vortex stretching and relative vorticity. On this boundary, $\psi = 0$ and isopycnals regain their reference depth ($\partial\psi/\partial z = 0$). Since the surface boundary condition is $\psi_z = 0$, the vertical integral of vortex stretching vanishes at the bowl.

These facts have been used by MN and Greatbatch (1987) to find the depth of this interface as a continuous function of latitude. The formulation of the problem is shown in Fig. 4. The potential vorticity is specified everywhere where there is flow as in the layer model above. The surface is at $z = 0$ and the low q water extends down to $z = -m$. The bowl is at $z = -D(y)$. There are three fixed boundaries with appropriate conditions while the bowl is a free boundary where extra information is needed to specify its position. If (2) is integrated vertically from $-D(y)$ to the surface, the vortex stretching term vanishes and one obtains

$$D = \frac{1}{|y|}\left[mL - \frac{1}{\beta}\frac{|y|}{y}\int_{-D}^{0}\nabla^2\psi dz\right]. \qquad (6)$$

If relative vorticity is neglected, then $D(y)$ simply follows the hyperbolic-plunge described by MN. Note that in this case, surprisingly, the depth profile is independent of stratification. A natural question to ask is: can the circulation really extend to infinite depths, and if not, does it reach the ocean floor? Near the eastward jet, the relative vorticity integral term in (6) becomes significant and positive, tending to make the bowl more shallow. It is conceivable that the penetration of the flow could be finite.

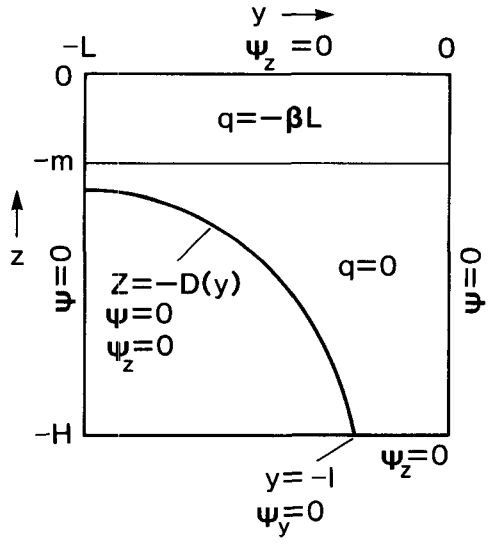

FIG. 4. The formulation of the free boundary problem. Potential vorticity is specified above the bowl and there is no flow below. Boundary conditions are applied to close the problem and locate the bowl.

To answer this question, the full problem must be solved by numerically inverting (2). An iterative approach has been used to find $D(y)$, in which $\psi = 0$ is imposed everywhere along the bowl and solutions are sought in which $\psi_z = 0$ is also satisfied. This was achieved by searching for vertical minima in the geostrophic energy (see appendix A). However, if it is the case that the bowl intersects the bottom, some method of finding the latitude of intersection, $y = -l$, must be employed. The position of the bowl is normally found through the knowledge that ψ and ψ_z are zero. If s is a coordinate along the direction of the bowl, then it follows from the chain rule that

$$\frac{\partial\psi}{\partial z}\frac{dz}{ds} + \frac{\partial\psi}{\partial y}\frac{dy}{ds} = 0$$

on any ψ contour, including the bowl. Since ψ_z is zero on the bowl, this implies that ψ_y is also zero on the bowl, provided only that the bowl is not vertical. So the natural choice for the southern boundary condition of the bottom flow is $\psi_y = 0$. In fact, this is the only condition which, when imposed at the ocean floor, can allow it to connect smoothly onto the free boundary above. It is consistent with the existence of stagnant water everywhere south of $y = -l$, while satisfying the extremum principle of CIY. Following Gill (1984) and Nurser (1988), a vertical profile was used for N to allow the stratification to diminish realistically with depth:

$$N = s/2h, \qquad z > -h$$
$$N = s/(h - z), \qquad z < -h \qquad (7)$$

where s and h are empirically derived constants (= 2.8 m s^{-1} and 150 m). Full details of the method of solution are given in appendix A.

3. Results

a. Inversions in a very deep ocean

In order to discover how deep the circulation could be expected to penetrate, Eq. (2) was inverted with realistic stratification, a meridional gyre extent of 1500 km and an upper low q layer 500 m deep. The values of f and β pertaining to latitude 40°N were used. The depth of the domain was allowed to become as large as necessary in order to prevent the bowl from hitting the bottom. Figure 5 shows the solution, which consists of a strong, surface intensified eastward jet with a weak, broad return flow to the south. Note that the y coordinates have been stretched so that the eastward jet region can be clearly seen (see appendix A). As suspected, the bowl does indeed "bottom out", the circulation penetrating to a depth of 10 km below the eastward jet. So it seems likely that the circulation extends to the bottom, although it must be stressed that

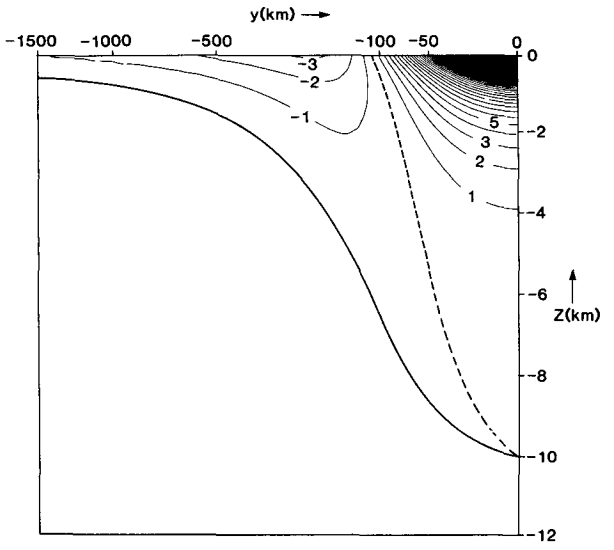

FIG. 5. Zonal velocity section from the solution for a deep ocean. The flow extends down to 10 km. The contour interval is 1 cm s^{-1} and the maximum eastward velocity is 79 cm s^{-1}. Note that the y coordinates have been stretched to emphasize the region of the eastward jet (see appendix A).

the penetration depth is dependent on the parameters used. Talley (1988) has presented evidence that in the Pacific, a relatively poorly ventilated ocean with a shallow main thermocline, the homogeneous q region extends only to 2½ km depth (although it is possible that it may penetrate deeper on a scale unresolved by these data).

Figure 6 shows how variations in the depth, m, of the upper layer affect the depth of penetration of the flow, D ($y = 0$). As expected the bowl gets deeper as the depth of the low q layer increases. In fact this relationship is one of simple proportionality. This can be understood by recognizing that at $y = 0$, (2) reduces to $q = \nabla^2\psi$. Substituting this into (6) leads to the proportionality of D to m. The other parameter which can be varied is the stratification, N^2. This becomes an important factor in determining both the strength of the flow and the depth of the bowl, because it sets the balance between the relative vorticity and vortex stretching terms [this should be compared with the analysis of section 2, where the value of N^2 has no effect on the penetration depth unless the relative vorticity term is included in (6)]. In the case where there is uniform potential vorticity in the upper layer, and the flow does not reach the ocean floor, the scale of the inertial boundary layer, $(U_I/\beta)^{1/2}$, is equal to the Rossby radius, L_ρ (see MN), which in turn depends on the stratification (U_I is a westward interior velocity scale). Figure 7 shows the dependence of the penetration depth on the (uniform) value of N^2. In a strongly stratified ocean, the boundary current becomes broader and the gyre circulates rapidly. In this case the bowl becomes very shallow as its penetration is inhibited beneath the relatively broad eastward jet. As N^2 is decreased, the Rossby radius is reduced and the eastward jet becomes narrower, so the penetration is only arrested farther north at deeper levels. The finite flow penetration results mainly from the action of relative vorticity at upper levels, allowing the isopycnal at the base of the upper layer to return to its reference depth at $y = 0$, as illustrated in Fig. 3. These results are consistent with layer model results (MN; Cessi 1988) which show that the width of the lower gyre is dependent on the strength of the upper forcing, the ratio of the layer depths and, in cases where the relative vorticity plays a role in determining the gyre width, the Rossby radius.

b. Inversions in an ocean of realistic depth

Given the likelihood of the flow penetrating to the ocean floor, it is interesting to investigate the form and meridional extent of the bottom currents and their effect on the structure and transport of the gyre above. We shall consider two regions of the model: In the core region, north of the latitude where the bowl hits the bottom ($y = -l$), a depth-independent flow is allowed, which can enhance the transport. South of $y = -l$ is a purely baroclinic fringe region.

A similar inversion to that of Fig. 5 is shown in Fig. 8 except that in this case the ocean is 5 km deep and the flow extends to the bottom. North of $y = -l$, the existence of a barotropic component is clear in the velocity field of Fig. (8a). But, in general, the depth-dependent form chosen for N^2 serves to concentrate the strongest flow near the surface. Figure 8b shows the potential vorticity field for reference and Fig. 8c shows

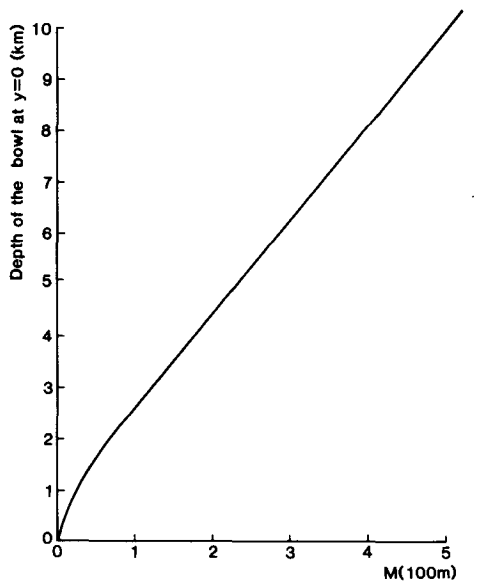

FIG. 6. Maximum depth of the bowl plotted against the depth of the surface (low q) layer (using realistic stratification).

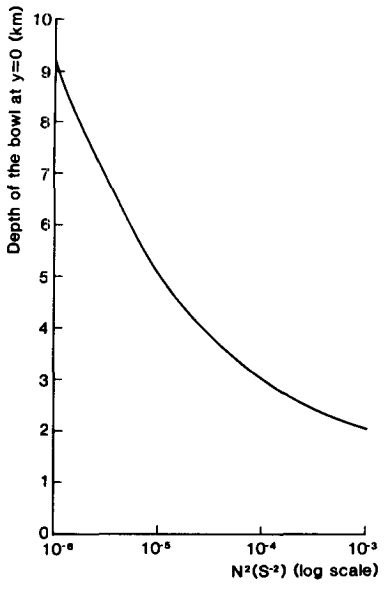

FIG. 7. Maximum depth of the bowl plotted against the stratification, with a surface layer 500 m deep. A vertically uniform N^2 has been used for these inversions.

the vortex stretching term. By comparing these two it can be seen that the stretching simply balances the beta effect over most of the southern, westward flowing part of the gyre. Vortex stretching is important at all depths, although it disappears in the vertical integral, with negative values above $z = -m$ canceling positive values below. Vortex stretching is the dominant dynamical process throughout the fringe and over significant regions of the core. Figure 8d shows the ratio of relative vorticity to vortex stretching; $\nabla^2\psi$ only dominates in the upper reaches of the eastward jet (it is in this region that isopycnals are brought back to their reference levels, arresting the depth penetration of the flow far below in the example of Fig. 5). However, while relative vorticity is small in absolute magnitude over much of the domain, it is crucial in controlling the structure of the recirculating core. Its importance relative to vortex stretching also has a minor peak in the deep flow at the southern edge of the core, where the no-slip boundary condition has been applied, implying a strong influence in the deep westward as well as eastward flow.

c. *Solutions for the barotropic mode*

In the core, north of $y = -l$, the depth integral of q does not vary with y (q is uniform in y for both the upper layer and the abyssal region). Therefore, since the depth integral of vortex stretching is zero, changes in planetary vorticity must be offset by relative vorticity in a depth integral sense. So integrating (2) vertically, it becomes

$$\tilde{q} = y + \phi_{yy} \tag{8}$$

where q has been scaled by βL, y by L and ψ by βL^3; ϕ is the depth average of ψ, the barotropic mode streamfunction, and $\tilde{q}$ is the depth average of q, equal to $-m/H$, where H is the depth of the ocean. Equation (8) has solution

$$\phi = -\frac{y^3}{6} + \tilde{q}\frac{y^2}{2} + \left[\tilde{q}\frac{l}{2} + \frac{l^2}{6} - \frac{\phi_F}{l}\right] y \tag{9}$$

if $\phi = 0$ at $y = 0$, and ϕ_F is the value of ϕ at $y = -l$. An additional boundary condition must be used to determine l. In general, l will satisfy the relation

$$\frac{l^3}{3} + \tilde{q}\frac{l^2}{2} - \tilde{u}_F l + \phi_F = 0 \tag{10}$$

obtained by differentiating (9) at $y = -l$ ($\tilde{u}_F = -\phi_y$ at $y = -l$). Differentiation of (9) also yields

$$y_{\max} = \tilde{q} + \left[\tilde{q}^2 + \tilde{q}l + \frac{l^2}{3} - \frac{2\phi_F}{l}\right]^{1/2} \tag{11}$$

where $y_{\max}$ is the position at which the depth integrated streamfunction is a maximum, $\phi_{\max}$, the barotropic mode transport. Assuming for simplicity that the baroclinic fringe can be neglected, i.e. $\phi_F = 0$ and that $\tilde{u}_F = 0$ we obtain:

$$l = -\frac{3}{2}\tilde{q}$$

$$\phi_{\max} = -\tilde{q}^3/12 \left(= \frac{2}{81} l^3\right). \tag{12}$$

Equation (12) recovers the results of CIY and Cessi (1988) expressing the mass transport in terms of l. Table 1 gives values for the total transport, the fringe transport, and the meridional extent of the core provided by the analysis above and from the numerical inversions. (Note that 1 Sv is equal to 10^6 m^3 s^{-1}). It can be seen that although the barotropic mode analysis cannot capture the total transport of the model, it provides a fair approximation. It is also clear from Table 1 that this analysis accounts for more than just the transport recirculated within the core itself ($\phi_{\max} - \phi_F$) with the value calculated for l greater than that found in the numerical inversion. In the latter, the fringe transport is in fact substantial, indicating that $\phi_F = \tilde{u}_F = 0$ is not an appropriate boundary condition at the southern edge of the core. For such quantities a boundary condition applied at $z = -H$ is not equivalent to a boundary condition on the depth integrated flow. If the values for ϕ_F and $\tilde{u}_F$ are taken directly from the numerical inversion then (10), (11) and (9) can be used to calculate greatly improved estimates for l and $\phi_{\max}$ in turn. These are also given in Table 1.

To provide an estimate for ϕ_F which is independent of the numerical inversions, the transport can be calculated within the baroclinic fringe region, where ψ_{yy} can be neglected. Thus (2) becomes

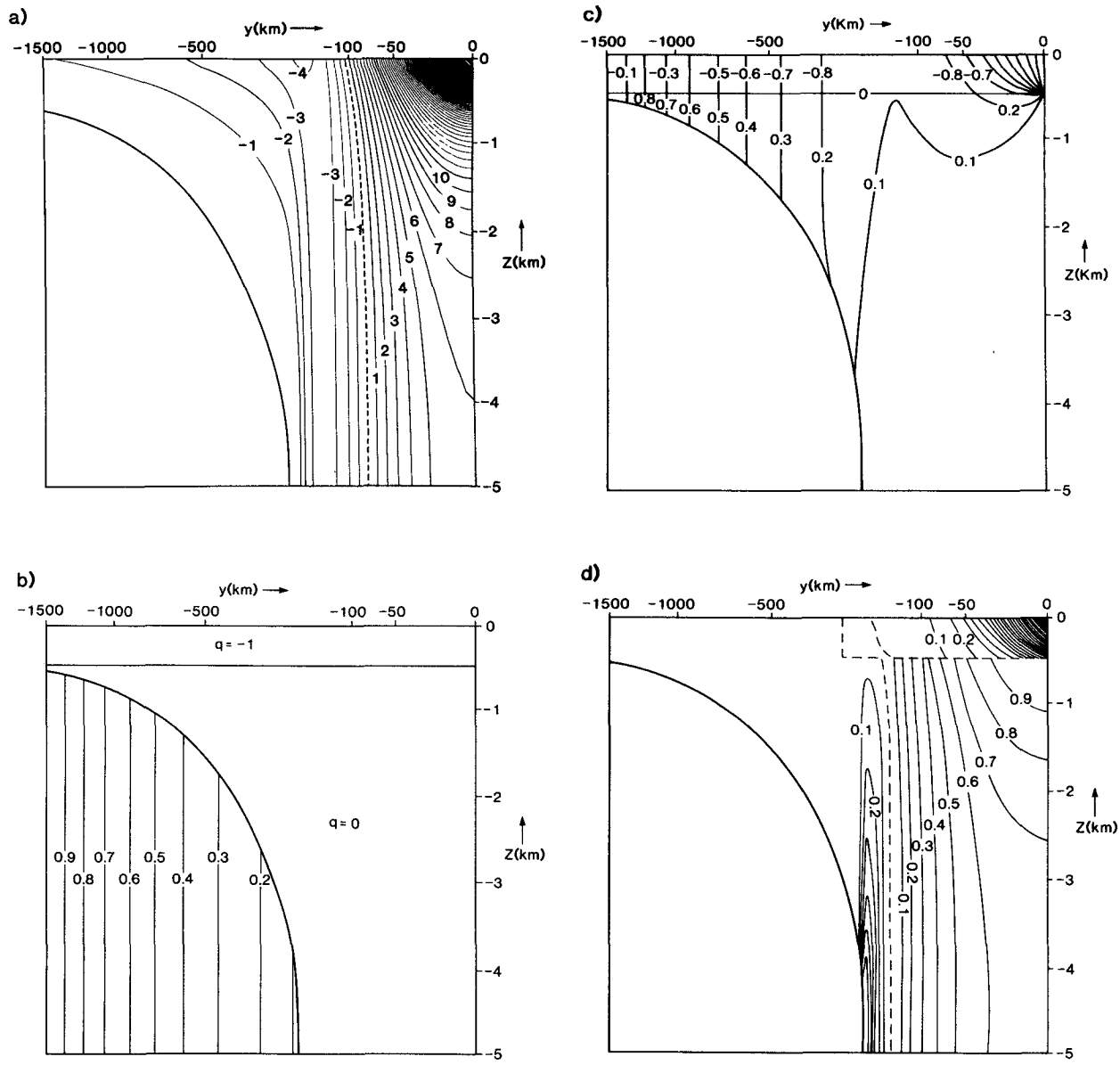

FIG. 8. An inversion in a 5-km-deep ocean with the bowl intersecting the bottom. The core region has a latitudinal extent of 206 km. (a) Zonal velocity (cm s^{-1}). Maximum eastward velocity is 82 cm s^{-1}; (b) Potential vorticity in units of βL; (c) the vortex stretching term in (2) in units of βL; (d) the ratio of relative vorticity to vortex stretching terms. y coordinates stretched as in appendix A.

$$F\psi_{zz} = q - y$$

where z is scaled by H and $F = (fL/NH)^2$ (constant stratification is assumed for simplicity). Solving this and integrating vertically, one obtains

$$\phi = \frac{m^3}{6F}\left[\frac{1}{y^2} - 1\right]$$

for the total fringe transport south of the latitude, y (m has been scaled by H). This gives an estimate for ϕ_F:

$$\phi_F \approx -\frac{\tilde{q}^3}{6Fl^2}.$$

Obviously this estimate is sensitive to the value chosen for the stratification; in fact, it is proportional to N^2. The depth average of N^2 for the profile given in (7) is 5.4×10^{-6} s^{-2} giving a value of 144 for F. Taking values of -0.1 for q and 0.2 for l this gives a conservative estimate of $\phi_F \sim 3 \times 10^{-5}$ or ~ 9 Sv. It is therefore reasonable to suppose that a significant proportion of the westward transport of the gyre can take place south of $y = -l$ in this case. Further details of the partition of transport between fringe and core will be presented in the next section, where it will be seen that these simple considerations of transport partition are

TABLE 1. A comparison of the barotropic mode solutions with the numerical inversions. Numbers in parentheses are taken directly from the numerical inversion and the corresponding value of $\tilde{u}_F$ used in the improved barotropic analysis was 2.38×10^{-4} in nondimensional units.

	$\phi_{max} \times 10^5$	ϕ_{max} (Sv)	$\phi_F \times 10^5$	ϕ_F (Sv)	l	l (km)
Barotropic analysis (Eq. (12))	8.33	23.9	—	—	0.15	225
Numerical inversion (Fig. (8))	10.10	29.0	4.60	13.2	0.1374	206.1
Improved barotropic analysis (Eqs. (9), (10) and (11))	9.98	28.7	(4.60)	(13.2)	0.1375	206.3

modified considerably when q varies with latitude, with the core gaining in importance as the overall transport is increased.

d. Inversions with a linear (q, ψ) relationship

The preceding analysis shows how the mass transport is controlled by the depth-integrated q, and to a large extent, the stratification. It is useful for comparing the model with theory, but the inferred transports are weak compared with eddy resolving quasi-geostrophic models and with observations. The potential vorticity of the thermocline is not uniform, but exhibits a marked minimum just south of the Gulf Stream. Therefore, if the model is to represent the recirculation accurately, it must be forced with a variable upper-layer q. In this section, following Greatbatch (1987) and MN2, we consider the effect of enhanced upper-layer forcing and bottom friction, as represented by the linear (q, ψ) relation in (3). MN2 presented a three-layer model with $dq/d\psi = c_1$ in the upper layer and c_3 in the third layer. We retain this notation but for the continuous model, c_1 is applied where $z > -m$ and c_3 decays exponentially upwards from the bottom with a height scale of 500 m.

Before assessing the effects of c_1 and c_3 on the transport of the model, we must first discuss the limits on their values. Application of the theory embodied in (4) (where Ekman dissipation replaces wind stress forcing for the lower layers) leads to the simple constraints: $c_1 \leqslant 0$; $c_3 \geqslant 0$. Further analysis of the interior flow in the three-layer model provides a limit on the strength of the upper forcing: $c_1 > -L_\rho^{-2}/2$ and also a lower limit on c_3. As pointed out by MN2, these limits are only meaningful if relative vorticity can be neglected. Such a boundary layer approximation is clearly inappropriate in the current model; the core is a few Rossby radii wide and c_3 has been set to zero in all the inversions presented so far. However, the limit on the magnitude of c_1 proves to be more relevant (the upper layer extends throughout the baroclinic fringe where relative vorticity is negligible). Indeed, as c_1 approaches a value of about $1200/L^2$, the matrix constructed from grid point "molecules" loses diagonal dominance and the inverter fails. An example of an inversion with nonzero $dq/d\psi$ is given in Fig. 9. The velocity and potential vorticity fields are shown with $c_1 = -800/L^2$ and $c_3 = |c_1| \exp[(z + H)/500]$. The transport is now 67 Sv, of which 42 Sv is depth independent.

The theory given in Greatbatch (1987) and MN2 shows that an increase in the magnitude of c_1 can be expected to increase the mass transport of the gyre, while increasing c_3 will inhibit the barotropic flow,

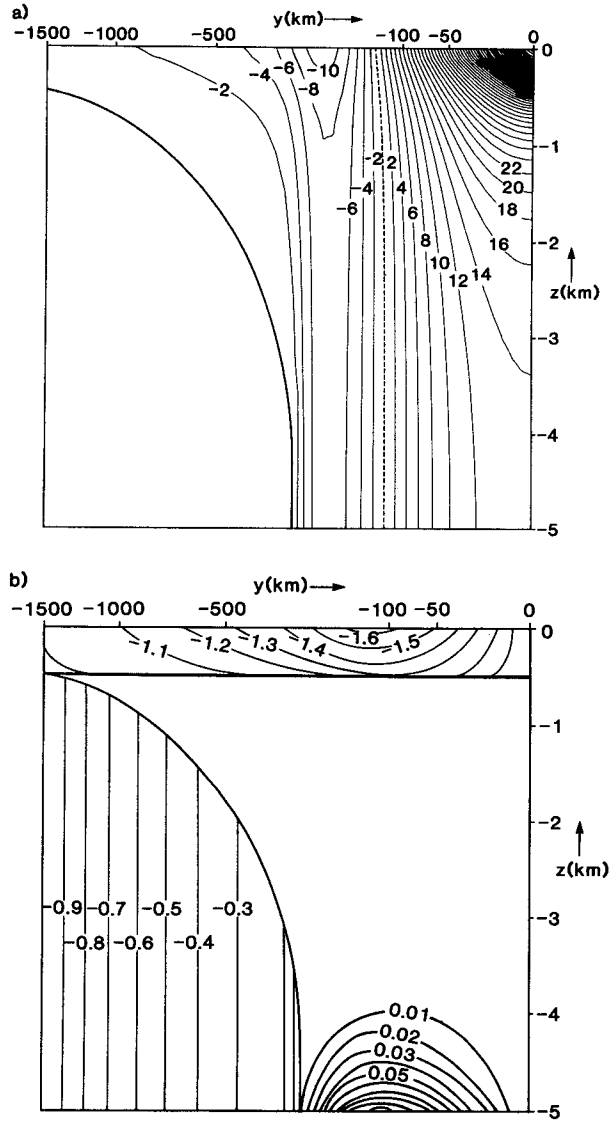

FIG. 9. As Fig. 8a,b, but with $c_1 = -800/L^2$ and $c_3 = |c_1| \exp[(z + H)/500]$. Maximum eastward velocity is 110 cm s^{-1} (note that the contour interval is now 2 cm s^{-1}). The core is 273 km wide. y coordinates stretched as in appendix A.

which is allowed when the gyre reaches the ocean floor. The present model has been used to study the influence of these parameters when relative vorticity is fully included. Figure 10 shows the dependence of the transport on c_1 and c_3. The transport has been split into two components: a purely baroclinic part, returned in the fringe (south of $y = -l$) and supplied by the surface intensified eastward jet, and the rest of the transport, returned within the core (north of $y = -l$) and almost exclusively barotropic in nature for all inversions carried out. Transport is plotted against the cube of the maximum magnitude of q in the upper layer. The linear dependence predicted in section 3c is still broadly adhered to. A value of $|q|^3_{\max} = 1$ obviously corresponds to $c_1 = 0$, and incremental changes in c_1 are denoted by tick marks on the curve, illustrating a rapid increase in transport as c_1 is increased. It can be seen immediately that the barotropic component, excited when the bowl hits the bottom, is a major contributor to the transport of the gyre. In general, as the magnitude of c_1 is increased, the proportion of the transport carried by the core also increases. This is because the core becomes both wider and more intense.

Two curves are shown: one has $c_3 = 0$ while the other has $c_3 = |c_1| \exp[(z + H)/500]$ (it is difficult to make an informed judgement on the relative magnitudes that c_1 and c_3 should have, but eddy resolving model results suggest that $|c_3|$ does not exceed $|c_1|$). It can be seen that nonzero c_3 causes the barotropic flow to become weaker. This is partly because the core has shrunk slightly and partly because the bottom flow has been retarded. But compared to the increase in transport effected by c_1, the decrease due to a corresponding value of c_3 is relatively small.

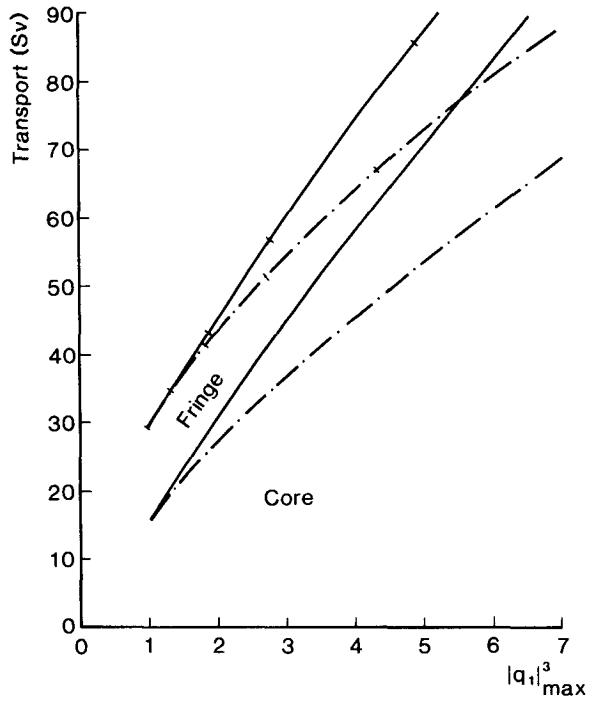

FIG. 10. Dependence of the transport on c_1 and c_3. Transport (Sv) is plotted against the cube of the maximum magnitude of the upper q (in units of βL). The curves represent the total transport and the component carried by the core for two cases: $c_3 = 0$ (solid lines) and $c_3 = |c_1| \exp[(z + H)/500]$ (dot-dashed lines) (the fringe transport is indicated as the difference between these curves). Tick marks denote increments of $200/L^2$ in the value of c_1.

If the model is to represent the total transport of the subtropical gyre, then the appropriate point to choose on the graph shown in Fig. 10 should correspond to a transport of ~75 Sv: the transport of one gyre in the eddy resolving numerical integrations carried out by Marshall et al. (1988, hereafter MNB). For this transport, c_1 takes a value of $\approx -800/L^2$, remarkably close to the value found by MNB when rescaled to their units. There are, however, differences between the inversions and the eddy resolving model. The flow in the inversions is more barotropic for this level of transport, with a wider, stronger core. This is partly due to a difference in the deep southern boundary condition. The no slip boundary condition on the southern edge of the deep westward flow is not appropriate for comparison with eddy resolving models such as that of MNB, in which the westward velocity does not decrease to zero at the gyre edge, but continues into an eddy driven, counterrotating cyclonic gyre to the south. This type of flow cannot be simulated by the inversions presented above. It should also be noted that the eddy resolving model has a quite different upper-layer potential vorticity profile with a stronger minimum in q and stronger gradients of q at the southern edge where q returns to a value of $-\beta L$. The similarity of values of c_1 for comparable transports arises from the combination of these two factors. Direct quantitative comparison of the two models is therefore more difficult than one might expect, especially with the transport so sensitively dependent on the depth integrated q.

Observational estimates for the transport of the recirculation vary considerably. In an analysis of the time-mean Gulf Stream at 55°W, Richardson (1985) estimates the eastward jet transport to be 93 Sv, of which 70 are recirculated locally (41 to the north and 29 to the south). One third of this transport is barotropic. Estimates of the synoptic transport (with which, perhaps, this model should be compared) are appreciably larger and current meter data (Hall and Bryden 1985) show the transport of the Gulf Stream to be 94 Sv and predominantly baroclinic at 68°W, *before* the onset of a barotropically intensified recirculation. Detailed comparison of the model results with observational data is difficult because of the idealized nature of the forcing and the restrictions of quasi-geostrophic theory. A model based on a more realistic equation set will be described in a subsequent contribution.

e. Summary

In summary, the model has been used to illuminate the vertical structure of the recirculation. Despite the apparent dominance of vortex stretching, relative vor-

ticity has been shown to be of importance, either in limiting the penetration depth or in controlling the depth integrated balance in the barotropic core. Both the overall transport of the gyre, and the partition of transport between barotropic and baroclinic components, has been shown to be dependent on the strength of the negative q anomaly in the upper layer. For a gyre with realistic transport, the barotropic component is greater but not predominant. It has been shown that bottom friction is capable of retarding the barotropic component of the flow, but has little effect on the overall transport compared to the considerable influence of imposing an upper (q, ψ) relationship of the same magnitude.

4. Inversions with anomalous deep potential vorticity

In the previous sections, the potential vorticity of the deep recirculating gyres has been assumed to be equal to the value of the planetary vorticity at the axis of the eastward jet. However, it is very unlikely that the entire deep homogeneous gyre should adhere strictly to this value of q. For example, it is well documented that the abyssal water of the western North Atlantic can have remote origins such as the Norwegian Sea (Hogg 1983) with very different values of f. Its potential vorticity is also likely to be influenced by convective and thermohaline processes at distant sites. These considerations are not directly related to the position of the Gulf Stream.

It is difficult to infer a value for the abyssal potential vorticity from hydrographic sections, which is appropriate to our idealized quasi-geostrophic model, although observations suggest that the abyssal anomaly is positive (see Fig. 3 of McCartney 1982, where the deep potential vorticity contours tend to swing southwards from the axis of the Gulf Stream into the abyss). In this section we will examine the sensitivity of the above solutions to changes in the deep q. It will be seen that the structure of the solution can be modified considerably by allowing the value of deep q to depart from our reference value and, also, that there is a limit on the strength of the abyssal q anomaly, above which solutions can no longer be found.

a. Influence on the extent and position of deep gyres

Since the forcing of the subtropical/subpolar gyre system is no longer antisymmetric, both gyres must now be considered together. Furthermore, it is no longer generally true that the latitude at which the upper layer streamfunction is equal to zero, marking the interface between the subtropical and subpolar gyres, is at $y = 0$. However, if potential vorticity is to be conserved in steady, free flow, this gyre interface must coincide with the front in potential vorticity, where q changes from a value of $-\beta L$ (subtropical gyre) to βL (subpolar gyre). This condition is therefore imposed in the models presented below; upper layer q is discontinuous and upper layer $\psi = 0$ at latitude $y = s$. The model formulation is shown in Fig. 11, with barotropic flow in the region $t < y < p$ and baroclinic fringes outside these latitudes.

The effect of a deep q anomaly on the shape of the bowl can be assessed by returning to Eq. (6). If a deep potential vorticity anomaly, $\gamma\beta L$ is assumed, where γ is a variable parameter, then (6) becomes

$$D = \left[mL\left(\frac{|y-s|}{y-s} - \gamma\right) - \frac{1}{\beta}\int_{-D}^{0} \nabla^2\psi dz \right] \Big/ (y - \gamma L)$$

For positive γ the bowl becomes deeper in the subpolar gyre and shallower in the subtropical gyre. If relative vorticity is neglected, the subpolar gyre now penetrates to infinite depth at $y = \gamma L$ and the solution for the depth of the bowl in the region $0 < y < \gamma L$ is not physically meaningful. However, relative vorticity cannot be neglected here, and furthermore, we expect the bowl to strike the bottom north of $y = \gamma L$ and south of $y = 0$. Since the subpolar gyre now becomes deeper and the sub-tropical gyre becomes more shallow, the latitudes at which the bowl strikes the bottom might be expected to migrate northwards. This phenomenon is investigated below.

b. Solutions for the barotropic mode and the two-layer problem

A similar analysis to that of section 3c can be carried out to discern the structure of the depth average flow in the core region, which now consists of two counter-rotating gyres. The solutions discussed below are essentially an extension of the solutions found by Cessi (1988) to the double gyre case with a nonzero value of q in the lower layer and an upper layer gyre interface at the variable latitude, $y = s$. Thus Eqs. (5) become

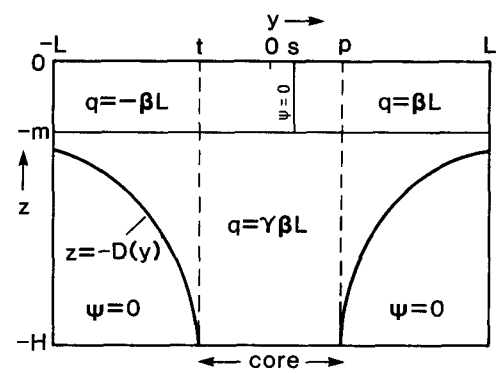

FIG. 11. Model formulation for the double gyre problem with nonzero deep potential vorticity and variable upper-gyre interface latitude. Boundary conditions as in Fig. 4.

$$\psi_{1yy} + y - q_1 + \left(\frac{L}{L_\rho}\right)^2(\psi_2 - \psi_1) = 0$$

$$\psi_{2yy} + y - \gamma + \alpha\left(\frac{L}{L_\rho}\right)^2(\psi_1 - \psi_2) = 0, \quad t < y < p \tag{13a}$$

with boundary conditions

$$\psi_1 = 0 \quad \text{at} \quad y = -1, s, 1$$

$$\psi_2 = 0 \quad \text{at} \quad y \leqslant t \quad \text{and} \quad y \geqslant p$$

$$\psi_{2y} = 0 \quad \text{at} \quad y = t, p \quad \text{(no slip)} \tag{13b}$$

and continuity of

$$\psi_2, \psi_{1y}, \psi_{2y} \quad \text{at} \quad y = s$$

where ψ has been scaled by βL^3, y by L and $q_1 = |y - s|/(y - s)$ The boundary conditions, (13b) are sufficient to solve (13a) and in addition, to determine the values of t, p and s. Projecting onto the barotropic and baroclinic modes,

$$\phi = (\alpha\psi_1 + \psi_2)/(1 + \alpha)$$

$$\theta = (\psi_1 - \psi_2)/(1 + \alpha).$$

Equations (13) can be rewritten as

$$\left.\begin{aligned}\epsilon^2[\psi_{1yy} + y - q_1] - \psi_1 = 0, \quad -1 \leqslant y \leqslant t;\ p \leqslant y \leqslant 1\\ \phi_{yy} + y - (q_1\alpha + \gamma)/(1 + \alpha) = 0\\ \epsilon^2[\theta_{yy} - (q_1 - \gamma)/(1 + \alpha)] - (1 + \alpha)\theta = 0\end{aligned}\right\}, \quad t < y < p \tag{14}$$

where $\epsilon = L_\rho/L$. Equations (14) can be solved for ϕ, the barotropic mode in the case where ϵ is small, i.e. the Rossby radius is much smaller than the gyre scale. This leads, through the imposition of the no-slip boundary conditions, to approximate solutions for t, p and s:

$$t = s - \frac{3\alpha}{2(1 + \alpha)} + O(\epsilon)$$

$$p = s + \frac{3\alpha}{2(1 + \alpha)} + O(\epsilon) \quad s = \frac{\gamma}{(1 + \alpha)} + O(\epsilon).$$

Note that $s < \gamma$, meaning that the deep q anomaly is truly positive relative to the latitude of the gyre interface. These solutions satisfy (14) to zero order in ϵ, at which $\psi_1 = \theta = 0$. Therefore the direct impact of a positive deep q anomaly on the depth average flow is to shift both the counter rotating gyres northwards, consistent with the analysis for the depth of the bowl offered above.

To assess the baroclinic response to the introduction of an abyssal q anomaly, higher order terms in ϵ must be considered. Using the following expansions

$$\psi_1 = \psi_{10} + \epsilon^2\psi_{11} + \cdots$$

$$\theta = \theta_0 + \epsilon^2\theta_1 + \cdots$$

for the upper level streamfunction in the fringes and the baroclinic mode in the core region respectively, immediately from (14) we have $\psi_{10} = \theta_0 = 0$. Using boundary layer approximations to match the interior solutions for these modes at $O(\epsilon^2)$, condition (13b) at $y = s$ yields

$$\phi = -\epsilon^2\theta_1 = -\frac{\epsilon^2\gamma}{(1 + \alpha)^2}\left(= \frac{\psi_2}{(1 + \alpha)}\right) \quad \text{at} \quad y = s$$

indicating that ψ_2 is negative for positive γ at $y = s$. The values of t, s and p can be found to $O(\epsilon^2)$. They are

$$t = s - \frac{3\alpha}{2(1 + \alpha)} - \frac{\alpha}{\omega}\epsilon + \left[\frac{8\gamma(1 + \omega)}{3\alpha^2} + \frac{2\chi}{3}\right]\epsilon^2 + O(\epsilon^3)$$

$$p = s + \frac{3\alpha}{2(1 + \alpha)} + \frac{\alpha}{\omega}\epsilon + \left[\frac{8\gamma(1 + \omega)}{3\alpha^2} - \frac{2\chi}{3}\right]\epsilon^2 + O(\epsilon^3)$$

$$s = \frac{\gamma}{(1 + \alpha)} - \frac{8\gamma(1 + \omega)}{9\alpha^2}\epsilon^2 + O(\epsilon^3) \tag{15}$$

where $\omega = 1 + \alpha + \sqrt{1 + \alpha}$ and $\chi = 6\alpha(1 + \alpha)/\omega^2 + (\alpha - 2)/\omega + 2(1 + \alpha)/\alpha$. It can further be calculated that the latitude, r, at which $\psi_2 = 0$, marking the interface between the abyssal gyres is given to $O(\epsilon^2)$ by

$$r = s - \frac{8\gamma(1 + \alpha)}{3\alpha^2}\epsilon^2 + O(\epsilon^3). \tag{16}$$

So the asymmetry between the abyssal gyres brought on by the deep potential vorticity anomaly, γ, only appears at $O(\epsilon^2)$, where an increase in γ effects an increase in both t and p, meaning that both gyres start to shift northwards *relative to latitude, s, of the upper-level gyre interface,* which is also shifting northwards. Furthermore, it can be seen that $r - s$ is negative at $O(\epsilon^2)$, implying that although the gyre interface moves northwards on increasing γ, it actually sweeps southwards with depth.

One can imagine a limit, for suitably baroclinic flows, at which the relative (to s) northward migration of the southern flank of the subtropical gyre (t) catches up with the relative southward migration of the abyssal gyre interface (r) resulting in the extinction of the deep subtropical gyre. Near this limit the Rossby radius scale boundary layers of the baroclinic mode at t and r interact and it becomes necessary to solve (13) without approximation. A numerical method has been used to obtain such solutions. Details are given in appendix B.

Consider first of all, the case when $\gamma = 0$. We find

that there are four exact solutions to the problem described by (13). One is trivial ($t = p = s$), one is symmetric ($t = -p$, $s = 0$) and two are asymmetric and complementary (in the sense that they map onto one another on rotation through half of a circle about the origin). Figure 12 shows the streamfunction and potential vorticity for the symmetric solution and one of the asymmetric solutions. The streamfunction shows the familiar double-gyre pattern in the symmetric case, but in the asymmetric cases, s is nonzero and there is only one lower gyre that occupies the entire region $t < y < p$. In the solution shown, s is positive and the deep gyre is cyclonic. In the other solution (not shown) s is negative and the deep gyre is anticyclonic. The potential vorticity in the symmetric case shows the imposed uniform value in the region $t < y < p$ in layer 2, with discontinuities at t and p. Outside this region it returns almost linearly to the value of the planetary vorticity at the edges of the domain. In contrast, the asymmetric solution shows closed q_2 contours in the stagnant region south of $y = t$. Invoking the extremum principle, we should expect these closed contours of potential vorticity to be eliminated by eddies, and hence the solution to relax back to the symmetric state. We argue, therefore, that it is only the symmetric, two-gyre solution which can be maintained physically.

Figure 13 shows the double-gyre solution with $\gamma = 0.25$ and $\alpha = \frac{1}{2}$. With $\gamma > 0$, again we find that the front in q_1 shifts northwards (note that $\gamma - s$ is again positive). However, it can now be seen that although the subtropical gyre has expanded in the upper layer, the subpolar gyre is dominant in layer 2, with the gyre interface moving southwards with depth. As before, there is one double-gyre solution, and two single (deep)-gyre solutions. As γ increases to about 0.39, the deep double-gyre becomes a single cyclonic gyre, which can be identified with the already existing single-gyre solution. At this limit, the merged solution has no extremum in q_2. If γ is increased beyond this point, then the solution disappears immediately and no solution to the problem can be found.

The upper limit on γ, γ_{max}, is sensitive to the other two parameters of the problem, L/L_ρ and α. Table 2 shows the values of γ_{max} as these parameters are varied. It can be seen that γ_{max} can take values ranging from very small to order unity. Also shown in this table is the width of a single lower-layer gyre and the ratio, R, of the maximum values of the streamfunction in the two layers, ψ_{2max}/ψ_{1max}. These latter two quantities are calculated for the symmetric ($\gamma = 0$) case. The quantity, R, is equal to zero for purely baroclinic flow and unity for barotropic flow. In some cases with a very small Rossby radius and/or a relatively shallow lower layer, identified by a — in the table, the deep subpolar gyre extends northwards to the edge of the domain before any limit in γ is encountered, so the idea of a limit on γ cannot be applied. In general, as the Rossby radius is increased the baroclinic mode becomes more important and γ_{max} decreases, implying a more stringent limit on the deep q anomaly. We also find that as the value of α becomes smaller, giving a deeper abyssal layer, the core region shrinks (as one would expect from the previous analysis) and the threshold value of γ is again reduced (for very small values of L/L_ρ and α the bottom flow disappears altogether). This can be understood in terms of Eqs. (15) and (16), which indicate that the tendency to extinguish one of the deep gyres depends on the quantity $\epsilon^2\gamma(1 + \alpha)/\alpha^2$. The existence of a limit on the deep potential vorticity anomaly is therefore observed for a moderate but realistic range of parameters, with the actual threshold value quite sensitive to these parameters. The response of the continuous model, with its standard parameters, to variations in γ will be examined in the next sections.

c. *Solution structure in the numerical inversions*

The behavior revealed above is also seen in the continuous model, in which a value of s was imposed and the value of γ gradually increased until precise correspondence between the upper-layer q front and gyre interface, given by $\psi = 0$, was achieved. In fact, the vertical structure of the flow was found to be very sensitive to γ, requiring this correspondence to be very accurate for consistent results. The results from a number of double gyre inversions show s and γ to be proportional as predicted in section 4b. The constant of proportionality is now slightly less than $(1 + \alpha)^{-1}$, or $(1 - m)$, due to asymmetry between the baroclinic fringes in accord with the expression for s given in (15). The values of t and p also increase linearly with γ. As s and γ are increased, the $\psi = 0$ contour, which marks the interface between the deep gyres, sweeps increasingly southwards with depth from the reference latitude, s.

Figure 14 shows an inversion in which the upper-layer q discontinuity has been moved north to $s = 0.177$ (corresponding to a shift of 265 km). The value of γ required to ensure conservation of upper-layer q was found to be 0.205. The usual boundary conditions have been applied to locate the bowl and to define the position of the core and for this figure the y coordinates have not been stretched. It can be seen that the entire deep homogenized region has shifted northwards together with the upper-layer gyre interface. The subtropical gyre has become larger and also shallower, while the subpolar gyre is deeper, and it is this cyclonic gyre that dominates the bottom flow, with the $\psi = 0$ contour sweeping southwards with depth. At the bottom it has been displaced almost to the southern edge of the core. This corresponds to the baroclinic structure seen in the two-layer model result of Fig. 13.

As γ is increased to about 0.225, the latitude where $\psi = 0$, between the two bottom gyres, becomes coincident with the southern extent of the bottom flow, and only one gyre remains. For higher values of s and γ, it becomes impossible to satisfy the additional boundary condition required, in order to specify this

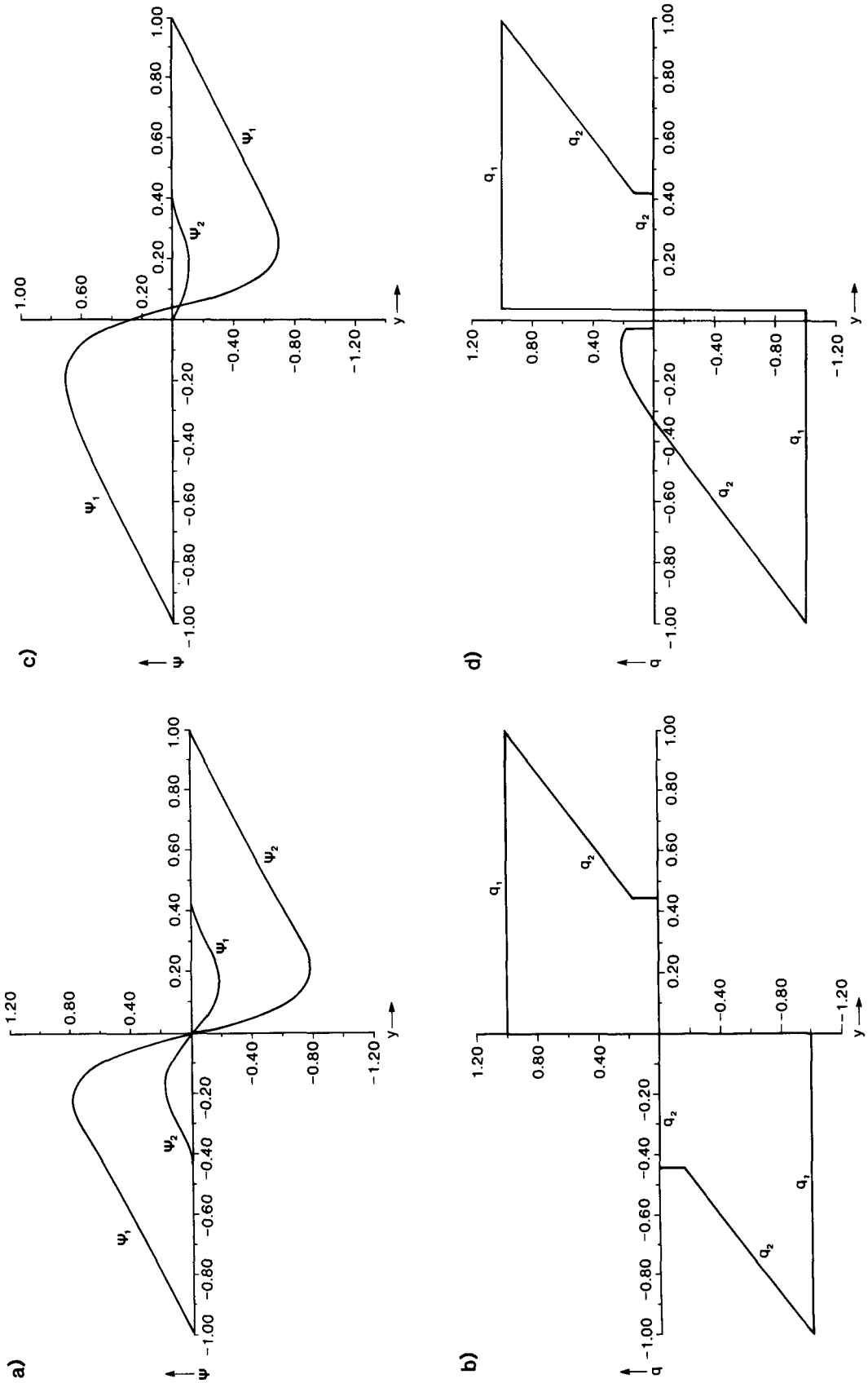

FIG. 12. Solutions to the two-layer double gyre problem with $\gamma = 0$, $\alpha = \frac{1}{2}$, $L/L_\rho = 10$. Streamfunction (in units of $\beta L_\rho{}^2 L$) and potential vorticity (in units of βL) are shown for the symmetric solution, (a) and (b), and the asymmetric solution with a single cyclonic deep gyre, (c) and (d).

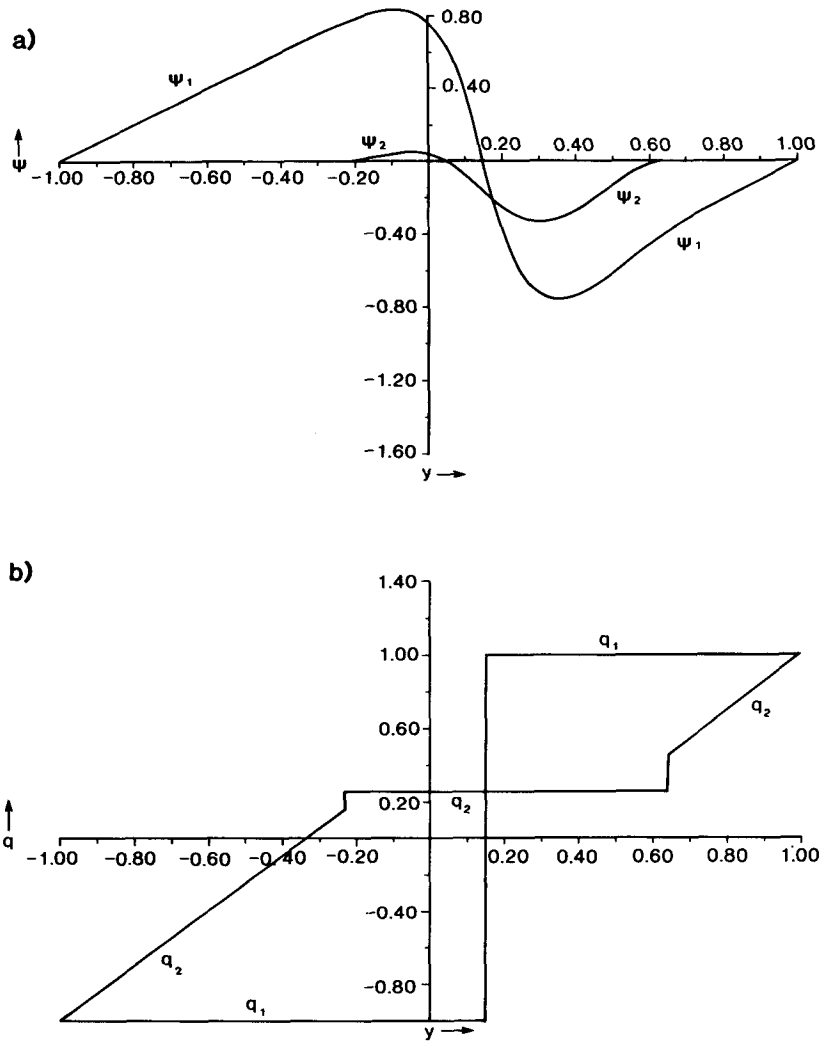

FIG. 13. Double deep-gyre solution corresponding to the solution shown in Fig. 12a,b but with $\gamma = 0.25$.

latitude. The horizontal iteration for the latitude at which the bowl strikes the bottom fails, and the southern extent of the core cannot be determined. This is analogous to the response of the two layer model to increasing γ, where the solution for layer 2 reached a single gyre state and then disappeared.

d. Discussion

The above analysis reveals that one can expect the strength, sense and position of the abyssal recirculation to show considerable dependence not only on the surface forcing, but also on the value assumed for the deep potential vorticity. If the perturbation is positive, as implied by the observations, then the upper-level gyre interface, together with the front in potential vorticity must migrate northwards. The deep flow region follows the northward shift, but the cyclonic gyre becomes stronger and more extensive than the anticyclonic gyre at depth. This result is in agreement with the abyssal recirculation scheme suggested by Hogg (1983) in which the subpolar gyre is dominant and the Gulf Stream sweeps southwards with depth.

The northward shift of the front in q can be explained in terms of a global integral constraint. If (2) is integrated over the domain of the model, we obtain

$$\int (q - \beta y) dA \approx m\Delta\bar{u} \tag{17}$$

where $\Delta\bar{u}$ is the difference between the average surface layer velocities at $y = L, -L$, the only latitudes where we do not have Neumann boundary conditions. If a positive deep q anomaly is introduced, then there must be an accompanying northward shift of the upper level discontinuity in order to preserve the right-hand side

TABLE 2. Parameter dependence of the two-layer model results. Three diagnostics are shown: γ_{max}; layer 2 single-gyre width, l_2, and the ratio, R, of the maximum values of the streamfunction in the two layers, ψ_{2max}/ψ_{1max}. The latter two quantities are for $\gamma = 0$.

	α				
	1	1/2	1/3	1/4	1/5
			$L/L_\rho = 7$		
γ_{max}	—	0.12	0.018	0.0035	0.00055
l_2	0.67	0.40	0.24	0.14	0.06
R	0.42	0.082	0.013	0.0016	0.00011
			$L/L_\rho = 10$		
γ_{max}	—	0.39	0.093	0.026	0.0080
l_2	0.70	0.45	0.31	0.22	0.15
R	0.64	0.23	0.067	0.019	0.0050
			$L/L_\rho = 15$		
γ_{max}	—	—	0.35	0.13	0.053
l_2	0.72	0.47	0.34	0.26	0.21
R	0.81	0.46	0.21	0.090	0.038
			$L/L_\rho = 20$		
γ_{max}	—	—	0.76	0.31	0.14
l_2	0.73	0.48	0.36	0.28	0.23
R	0.89	0.62	0.36	0.19	0.098
			$L/L_\rho = 25$		
γ_{max}	—	—	—	0.57	0.28
l_2	0.74	0.49	0.36	0.28	0.23
R	0.93	0.73	0.48	0.29	0.17

of (17) at a physical value. If there were no northward shift, an anomaly of $\gamma \sim 0.1$ would require this term to be orders of magnitude too large. It is clear from (17) that the northward shift in the front is dependent on the fact that the boundaries of the upper level gyres are fixed at $y = L, -L$. It could be argued that this assumption is artificial and that the boundaries of the domain should also be determined by application of further boundary conditions. This would, of course, render the problem trivial, simply shifting the origin to $y = \gamma L$. A more reasonable alternative would be to assume that the position of the eastward jet is prescribed at a fixed latitude, allowing the domain to mutate to accommodate (17). In terms of the baroclinic structure of the flow, this option is probably equivalent to the one pursued above.

The southward migration of the axis of the eastward jet with depth is also consistent with a positive deep q anomaly. The slope of a ψ contour is given by

$$\left(\frac{dz}{dy}\right)_{\psi\text{const}} = -\frac{\psi_y}{\psi_z}$$

and if the abyssal gyre interface is to slope southwards with depth, this quantity must be positive for the zero ψ contour. Now in the deep regions of the core, the vortex stretching term in (2) is greater in magnitude than the relative vorticity (see Fig. 8) and will therefore have the same sign as $q - \beta y$. Since the bottom boundary condition is $\psi_z = 0$, ψ_z will also have this sign. Therefore, provided the flow is eastward, a positive deep q anomaly (relative to the latitude, s) is likely to induce a southward slope of the zero ψ contour with depth.

Finally, it is significant that in the case where $\gamma \neq 0$, solutions can only be found when the zero ψ contour hits the bottom. As γ is increased, the southern edge of the core moves northwards and the subtropical gyre becomes smaller. At a critical value of γ, the zero ψ contour hits the bottom at the southern edge of the core. For larger values of γ there is no solution. This is because it is impossible for the zero ψ contour to intersect the bowl south of $y = t$. In general, a zero ψ contour cannot strike a free boundary (a zero streamline on which the first normal derivative of the streamfunction is zero) except at a point where the forcing changes sign along that boundary. This result can be proved by means of a Taylor expansion for ψ about a point on the free boundary (P. Cessi, personal communication 1987). Therefore, the only latitude at which the $\psi = 0$ contour is allowed to meet the bowl is at $y = \gamma L$, where $q - \beta y$ changes sign. However, if this contour slopes southward from $y = s$ and $s < \gamma L$, the above condition cannot be satisfied. In the case where $\gamma = 0$, the $\psi = 0$ contour may strike the bowl at $y = 0$, but if the abyssal potential vorticity is nonzero, then this can not happen and the flow in both gyres must extend to the bottom. It appears, therefore, that the symmetrical subpolar/subtropical gyre system, in

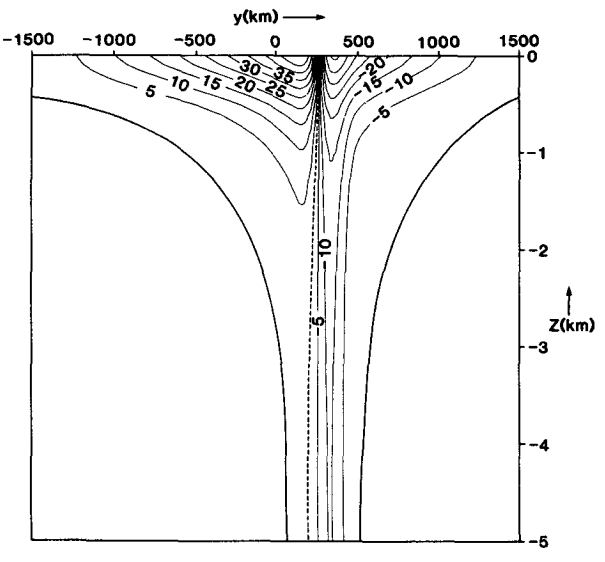

FIG. 14. Streamfunction, ψ, (in units of βL^3) from a double-gyre inversion with a deep q anomaly: $\gamma = 0.205$; $s = 0.177$ (=265 km); $c_1 = c_3 = 0$; the widths of the subpolar and subtropical gyres are 330 and 65 km, respectively, at the bottom. y coordinates are not stretched.

which the bowl bottoms out, is a singular case, for which asymmetries in the potential vorticity field cannot be supported. However, if the homogenized region extends to the bottom, the model is more robust, and can produce realistic asymmetric solutions.

In reality, bottom currents are observed in the recirculation regions of both the Atlantic and Pacific oceans. In the Pacific the bottom currents do not appear to relate systematically to the flow above, and probably owe their existence to processes not addressed in our simple model. The bottom currents in the Atlantic, on the other hand, appear to have some qualitative agreement with the above solutions, with a dominant cyclonic gyre at depth. The explanation offered above depends on the idea of positive potential vorticity anomalies being transported to the region from distant sites at least in the creation if not the maintenance of the steady state described by the model. The larger scale abyssal flow is certainly capable of this (see McDowell et al. 1982) and even though the process of potential vorticity injection into gyres which circulate within closed free streamlines can not be simulated in a steady state model, it should not be ruled out.

An alternative model of the deep cyclonic flow is given by Hogg and Stommel (1985), who simulate the abyssal recirculation in terms of uniform potential vorticity flow beneath a thermocline which surfaces. The latitudinal variation of their abyssal layer thickness implies that in order to conserve mass they must also have a positive deep potential vorticity anomaly with cyclonic deep flow beneath the Gulf Stream. In the alternative offered here, the deep potential vorticity anomaly is imposed, rather than deduced from the gross features of the vertical extent of the deep water, and both layers adjust to accommodate it. The conclusion of deep cyclonic flow is still reached if a small positive anomaly is assumed.

5. Conclusion

A diagnostic model has been presented, offering an interpretation of the current systems observed in the northwestern corners of the world's oceans in terms of idealized potential vorticity distributions. Almost free flow is assumed above the main thermocline, and a low value of potential vorticity is imposed in order to depress the main thermocline and represent mode water south of the Gulf Stream front. Homogeneous potential vorticity has been assigned to the abyssal flow. A model built on these assumptions can capture the essential character of the vertical and meridional structure of the recirculation regions, as revealed by hydrographic and current meter measurements. The emphasis has been on diagnosis of steady, free states, rather than on forcing mechanisms and their role in creating and maintaining these flow patterns.

First, it has been shown that the abyssal flow has a finite depth penetration, and that for oceanographic parameters this flow may not reach the bottom. This is a consequence of relative vorticity, which must be present to close any type of Fofonoff gyre. Such a process may account for the shallow region of homogeneous potential vorticity observed in the Pacific, although there are bottom currents in this region that require further explanation. It should be pointed out again that these solutions are not robust to small perturbations to the value of homogeneous potential vorticity.

In regimes with stronger surface forcing, or weaker stratification, the homogeneous flow penetrates to the ocean floor. The immediate consequence of this is the emergence of a strong barotropic component to the flow. The existence of this barotropic component allows us to define a partition in the mass transport of the model, between the depth-independent part, and the contribution made due to velocity shear from the bottom upwards. It has been found that there is close correspondence between this partition and a spatial partition which demarkates the transport into core and fringe regions. The eastward jet is very surface intensified, but the recirculation immediately to the south is only weakly depth dependent, the baroclinic part of the jet being recirculated farther south in the fringe where there are no bottom currents. The precise partition of transport between fringe and core depends on a number of factors. Again the degree of surface forcing is important with more strongly forced flows tending to be more barotropic. The strength of the stratification also has some bearing on this balance with stronger stratification tending to enhance the baroclinic component. To achieve a realistic transport in the region of 70 Sv, the maximum magnitude of upper-layer q must be $\sim 1.6\beta L$. In this case the core carries approximately 2½ times the transport of the fringe.

The novel feature of the work has been the full inclusion of both relative vorticity and vortex stretching components of the potential vorticity in a vertically continuous model. An ability to study the importance of these two terms has led to two conclusions:

1) The vortex stretching term is dominant in magnitude over almost the whole of the recirculation, although it disappears in vertical integral.

2) The relative vorticity term is vital, either in arresting the depth penetration of the flow, or in cases where bottom flow exists, in controlling the depth integral structure over the whole of the barotropic core of the recirculation. The inversions generally demonstrate that a decaying boundary layer type structure is not applicable to the barotropic core.

Finally, these free, homogeneous recirculation systems show some sensitivity to the value chosen for the abyssal potential vorticity. As the deep q anomaly becomes more positive, it is necessary for the upper level front in potential vorticity to move northwards together with the interface between the two gyres. The abyssal

flow region also shifts northwards, while the axis of the eastward jet sweeps southwards with depth. Therefore, although the subtropical gyre has expanded at the surface, the subpolar gyre is dominant at depth. Furthermore, we have seen that solutions can only be found so long as there are two counterrotating gyres at the bottom. There is an upper limit on the possible magnitude of the deep q anomaly, which corresponds to the expansion of one of these gyres to a point where it just fills the bottom flow region. The solutions shown in section 4 are suggestive of the deep flow in the western North Atlantic and although the model is again steady and diagnostic, and does not address the question of the creation or maintenance of these flow patterns, there is circumstantial evidence of a positive deep q anomaly and ample opportunity for maintaining it in the deep North Atlantic circulation.

The quasi-geostrophic framework of the model is its chief limitation, making quantitative comparison with observed potential vorticity distributions and hydrographic sections difficult. Extensions of the present work to an isopycnal model will be described in a subsequent contribution. There is further potential to extend the work to include the east–west dimension, and to study the effects of ventilation and bottom topography.

Acknowledgments. I would like to thank John Marshall and George Nurser for their help and advice. I am also grateful to Paola Cessi and another anonymous reviewer for criticisms and suggestions which have been of great benefit to the manuscript. This work was supported by the Natural Environment Research Council of the United Kingdom.

APPENDIX A

Numerical Details for the Inversions

1. The iteration scheme

The potential vorticity field is inverted with a free boundary (the bowl) specified at each grid point position in the horizontal and between grid points in the vertical. It is known that on this boundary, and on all grid points below it, $\psi = 0$ (see Fig. 4). In general, the boundary will cut between grid points in the horizontal and in the vertical, and this is taken into account in the finite differencing above the boundary. Consider the situation in Fig. (15). A set of grid points is shown with the bowl passing between them. Outlying values of ψ can be expressed as Taylor expansions about the central grid point where $\psi = \psi_0$:

$$\psi_+ = \psi_0 + l\psi_{y0} + \frac{l^2}{2}\psi_{yy0} + O(l^3)$$

$$0 = \psi_0 - \alpha l\psi_{y0} + \frac{\alpha^2 l^2}{2}\psi_{yy0} + O(l^3).$$

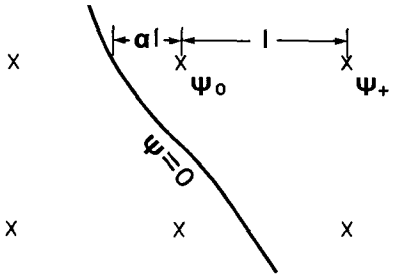

FIG. 15. Grid points in the numerical inversion with the bowl passing between them.

Subscripts denote grid point positions as in Fig. (15), l is the nondimensional grid spacing and α is the fraction of l shown in Fig. (15). These expansions lead to the following finite difference representations for first and second derivatives at the central grid point:

$$\psi_{y0} = \frac{1}{\alpha(1+\alpha)l}[\alpha^2\psi_+ + (1-\alpha^2)\psi_0] + O(l^2)$$

$$\psi_{yy0} = \frac{2}{\alpha(1+\alpha)l^2}[\alpha\psi_+ - (1+\alpha)\psi_0] + O(l).$$

These are used to calculate quantities on grid points just above the boundary.

The extra condition that must be satisfied at the bowl is $\psi_z = 0$. As discussed in section 3b, ψ_y must also be zero at each point on the bowl thus we can form the following quantity,

$$\frac{1}{2}(\psi_y)^2 + \frac{f_0^2}{N^2}(\psi_z)^2 \quad (= \text{KE} + \text{APE}),$$

which must be zero on the bowl. This quantity has the desirable properties of being positive definite and nonzero everywhere except on the bowl. It is minimized just above each individual boundary point in the following way: Contours of a vertical minimum are found and the position of the bowl moved up to meet these minima in decreasing increments. It was necessary to sweep inward from the edges of the gyres towards $y = 0$, while iterating upward for the bowl, because the vertical positions of the energy minima near the eastward jet are sensitive to the solution in the interiors of the gyres. The iteration stops when the bowl sits just below an energy minimum at each horizontal grid position. Ideally, this quantity should be zero on the bowl, and it was found to be negligible in all cases once the bowl had been located to grid point accuracy. For cases where the bowl intersects the bottom, a similar procedure was followed to find the latitudes bounding the core. The position at which the bowl intersected the bottom was moved inwards towards $y = 0$ until the required lateral boundary condition ($\psi_y = 0$) was satisfied to within one grid point.

2. The coordinate stretching

It was necessary to use an irregular grid to provide the model with sufficient resolution in the eastward flow region. The following expression was used:

$$y = 5u - 5.9253 \tanh(0.82u)$$

where y, and u are the nondimensional northward coordinates in physical space and grid space, respectively. The numbers have been chosen such that the function is monotonic; with finite derivatives at the boundaries; with y and u equal at -1, 0 and 1 and able the stretch the middle of the double gyre in a continuous manner.

APPENDIX B

Solution of the Two-Layer Double Gyre Model

Equations (13) have the following solutions in four different regions:

$$-1 \leqslant y \leqslant t: \quad \psi_1 = y + 1 + A \sinh[(y+1)/\epsilon]$$

$$\psi_2 = 0$$

$t \leqslant y \leqslant s$:

$$\alpha\psi_1 + \psi_2 = -\lambda^2\left[\frac{y'^3}{6} + \left\{\frac{\alpha-\gamma}{1+\alpha} + s\right\}\frac{y'^2}{2} + By' + C\right]$$

$$\psi_1 - \psi_2 = \left(\frac{1+\gamma}{1+\alpha}\right)[1 - \cosh\lambda y'] + \lambda^2 C \cosh\lambda y' + (1+\alpha)D \sinh\lambda y'$$

$s \leqslant y \leqslant p$:

$$\alpha\psi_1 + \psi_2 = -\lambda^2\left[\frac{y'^3}{6} - \left\{\frac{\alpha+\gamma}{1+\alpha} - s\right\}\frac{y'^2}{2} + By' + C\right]$$

$$\psi_1 - \psi_2 = \left(\frac{\gamma-1}{1+\alpha}\right)[1 - \cosh\lambda y'] + \lambda^2 C \cosh\lambda y' + (1+\alpha)D \sinh\lambda y'$$

$$p \leqslant y \leqslant 1: \quad \psi_1 = y - 1 + E \sinh[(y-1)/\epsilon]$$

$$\psi_2 = 0$$

where $y' = y - s$, $\epsilon = L_\rho/L$, $\lambda = (1+\alpha)^{1/2}\epsilon^{-1}$, ψ has now been scaled by $\beta L_\rho{}^2 L$ and y by L. The above solutions yield $\psi_1 = 0$ at $y = 1, -1, s$ and ψ and ψ_y are matched at $y = s$ in both layers.

Application of the further conditions that the normal modes, and their first derivatives must match at $y = t$, p produces eight equations in the five arbitrary constants, A to E, and cubic and hyperbolic functions of t, p and s. Five of these equations were used in a linear inversion to find the values of A to E. These values were then used in the other three equations to provide three residual functions which were then minimized by varying t, p and s (each time recalculating A to E). Mutual zeros of these three residual functions correspond to the four types of solutions for t, p and s referred to in the text.

REFERENCES

Cessi, P., 1988: A stratified model of the inertial recirculation. *J. Phys. Oceanogr.*, **18**, 662–682.

——, G. R. Ierley and W. R. Young, 1987: A model of the inertial recirculation driven by potential vorticity anomalies. *J. Phys. Oceanogr.*, **17**, 1640–1652.

Fofonoff, N. P., 1954: Steady flow in a frictionless homogeneous ocean. *J. Mar. Res.*, **13**, 254–262.

Gill, A. E., 1984: On the behavior of internal waves in the wakes of storms. *J. Phys. Oceanogr.*, **14**, 1129–1151.

Greatbatch, R. J., 1987: A model for the inertial recirculation of a gyre. *J. Mar. Res.*, **45**, 601–634.

Hall, M. M., and H. L. Bryden, 1985: Profiling the Gulf Stream with a current meter mooring. *Geophys. Res. Lett.*, **12**, 203–206.

Hogg, N. G., 1983: A note on the deep circulation of the western North Atlantic: Its nature and causes. *Deep-Sea Res.*, **30**, 945–961.

——, and H. Stommel, 1985: On the relation between the deep circulation and the Gulf Stream. *Deep-Sea Res.*, **32**, 1181–1193.

Keffer, T., 1985: The ventilation of the world's oceans: Maps of the potential vorticity field. *J. Phys. Oceanogr.*, **15**, 509–523.

Marshall, J. C., and A. J. G. Nurser, 1986: Steady free flow in a stratified quasi-geostrophic ocean. *J. Phys. Oceanogr.*, **16**, 1799–1813.

——, and ——, 1988: On the recirculation of the subtropical gyre. *Quart. J. Roy. Meteor. Soc.*, **114**, 1517–1534.

——, —— and R. Brugge, 1988: On the time mean flow of quasi-geostrophic wind driven gyres. *J. Geophys. Res.*, **93**, 15427–15436.

McCartney, M. S., 1982: The sub-tropical recirculation of mode waters. *J. Mar. Res.*, **40**(Suppl), 427–464.

McDowell, S., P. B. Rhines and T. Keffer, 1982: North Atlantic potential vorticity and its relation to the general circulation. *J. Phys. Oceanogr.*, **12**, 1417–1436.

Niiler, P. P., 1966: On the theory of wind driven ocean circulation. *Deep-Sea Res.*, **13**, 597–606.

Nurser, A. J. G., 1988: The distortion of a baroclinic Fofonoff gyre by wind forcing. *J. Phys. Oceanogr.*, **18**, 243–257.

Rhines, P. B., and W. R. Young, 1982a: Homogenization of potential vorticity in planetary gyres. *J. Fluid Mech.*, **122**, 347–367.

——, and ——, 1982b: A theory of the wind driven ocean circulation. Part I: Mid-ocean gyres. *J. Mar. Res.*, **40**(Suppl), 559–596.

Richardson, P. L., 1985: Average velocity and transport of the Gulf Stream near 55 W. *J. Mar. Res.*, **38**, 111–135.

Talley, L. D., 1988: Potential vorticity distribution in the North Pacific. *J. Phys. Oceanogr.*, **18**, 89–106.